Biophysical Journal
Article

Biophysical Society

The Charge Properties of Phospholipid Nanodiscs

Cheng Her,[1,*] Dana I. Filoti,[1] Mark A. McLean,[2] Stephen G. Sligar,[2] J. B. Alexander Ross,[3] Harmen Steele,[2] and Thomas M. Laue[1]

[1]Department of Molecular, Cellular and Biomedical Sciences, University of New Hampshire, Durham, New Hampshire; [2]Department of Biochemistry, University of Illinois at Urbana-Champaign, Champaign, Illinois; and [3]Department of Chemistry and Biochemistry, University of Montana, Missoula, Montana

ABSTRACT Phospholipids (PLs) are a major, diverse constituent of cell membranes. PL diversity arises from the nature of the fatty acid chains, as well as the headgroup structure. The headgroup charge is thought to contribute to both the strength and specificity of protein-membrane interactions. Because it has been difficult to measure membrane charge, ascertaining the role charge plays in these interactions has been challenging. Presented here are charge measurements on lipid Nanodiscs at 20°C in 100 mM NaCl, 50 mM Tris, at pH 7.4. Values are also reported for measurements made in the presence of Ca^{2+} and Mg^{2+} as a function of NaCl concentration, pH, and temperature, and in solvents containing other types of cations and anions. Measurements were made for neutral (phosphatidylcholine and phosphatidylethanolamine) and anionic (phosphatidylserine, phosphatidic acid, cardiolipin, and phosphatidylinositol 4,5-bisphosphate (PIP_2)) PLs containing palmitoyl-oleoyl and dimyristoyl fatty acid chains. In addition, charge measurements were made on Nanodiscs containing an *Escherichia coli* lipid extract. The data collected reveal that 1) POPE is anionic and not neutral at pH 7.4; 2) high-anionic-content Nanodiscs exhibit polyelectrolyte behavior; 3) 3 mM Ca^{2+} neutralizes a constant fraction of the charge, but not a constant amount of charge, for POPS and POPC Nanodiscs; 4) in contrast to some previous work, POPC only interacts weakly with Ca^{2+}; 5) divalent cations interact with lipids in a lipid- and ion-specific manner for POPA and PIP_2 lipids; and 6) the monovalent anion type has little influence on the lipid charge. These results should help eliminate inconsistencies among data obtained using different techniques, membrane systems, and experimental conditions, and they provide foundational data for developing an accurate view of membranes and membrane-protein interactions.

INTRODUCTION

Charge is a fundamental property that directly influences the structure, stability, solubility, and interactions of macromolecules (1,2). Since the solution electrostatic properties of a molecule are affected by the solvent composition (i.e., ionic strength, ion type, etc.), pH, dielectric constant, and temperature, charge is a system property. Charge estimates based on amino acid sequences (3,4), nucleotide sequences (5–7), and lipid headgroups (8) are typically higher in magnitude than their experimental counterparts. The discrepancy between calculations and measurements for proteins seems to result from the failure of calculations to consider ion binding aside from H^+ (4), whereas for nucleic acids, polyelectrolyte behavior reduces the charge (7). Although good charge measurement data are available for proteins and nucleic acids (8,9), obtaining charge measurements in lipids has posed experimental difficulties. This lack of solid charge information is unfortunate because the membrane composition, including charge, is of fundamental importance for a variety of cellular and physiological functions (10).

Lipids, in the form of liposomes, have been difficult to analyze electrophoretically due to their tendency to aggregate and their interactions with glass (11). Two advances have made lipid charge measurements feasible. First, lipid Nanodiscs provide a stable membrane platform that is suitable for electrophoretic charge measurements (12). Nanodiscs are composed of a phospholipid (PL) bilayer stabilized by a pair of membrane scaffolding proteins (MSPs) that act like a belt around the lipid bilayer (13). These MSPs are negatively charged and provide enough electrostatic repulsion to prevent the Nanodiscs from aggregating in standard buffer. In addition, the MSPs allow the migration of the Nanodiscs to be monitored using UV optics. Second, membrane-confined electrophoresis (MCE) has been shown to provide accurate charge measurements on macromolecules in physiological solvents using small quantities of material (7,14,15). In this work, we took advantage of these two advances to obtain the first, to our knowledge, systematic measurements of lipid charge.

Submitted November 13, 2015, and accepted for publication June 15, 2016.

*Correspondence: ccd35@wildcats.unh.edu

Editor: Ka Yee Lee.

http://dx.doi.org/10.1016/j.bpj.2016.06.041

These data will help refine hypotheses and improve the accuracy of lipid membrane models (16,17).

Because the nomenclature for charge measurement is complicated, and because there are a number of derived quantities, a glossary of terms is included in Table 1. It should be noted that the terms "charge" and "valence" have been used interchangeably, even though all of the results are reported as valences.

MATERIALS AND METHODS

Nanodiscs

Nanodiscs were obtained from Dr. Mark McLean of the Sligar group at the University of Illinois at Urbana-Champaign, and Harmen Steele of the Ross group at the University of Montana. We used two types of MSPs: MSP1D1, which holds ~126 lipids (63 per monolayer), and MSP1E3D1, which holds ~250 lipids (125 per monolayer (12)). The initial concentrations of 1-palmitoyl-2-oleoyl-*sn*-glycero-3-phosphocholine (POPC), 10% palmitoyl-oleoyl phosphatidylserine (POPS), 30% POPS, and 70% POPS (referred to as 10POPS, 30POPS, and 70POPS, respectively) MSP1D1 and MSP1E3D1 Nanodiscs were ~20 μM. The initial concentrations of MSP1D1 10% POPC-1-palmitoyl-2-oleoyl-*sn*-glycero-3-phosphate (POPA), 30% POPA, and 70% POPA Nanodiscs (referred to as 10POPA, 30POPA, and 70POPA, respectively) were ~10 μM. The initial concentrations of MSP1D1 10% 1-palmitoyl-2-oleoyl-*sn*-glycero-3-phosphoethanolamine (POPE) and 10% phosphatidylinositol 4,5-bisphosphate (PIP_2; referred to as 10POPE and 10PIP_2, respectively) Nanodiscs were ~8 μM. Nanodiscs were prepared in 100 mM NaCl, 50 mM Tris, pH 7.4, containing 0.1% NaN_3. Initially, stock solutions of Nanodiscs were dialyzed against a standard solvent (lacking NaN_3) for 3 days, with three solvent exchanges per day (at a volume of 5000:1) using Slide-A-Lyzer Dialysis Cassettes (ThermoFisher Scientific, Waltham, MA). However, no significant charge difference was observed after only 8 h of dialysis, and this shorter dialysis time was used routinely. When used, the samples were dialyzed in standard solvent containing either 3 mM $CaCl_2$ or 3 mM $MgCl_2$ added.

MCE

All measurements were carried out in an MCE apparatus (Spin Analytical, Berwick, ME) in standard buffer or standard buffer containing 3 mM Ca^{2+} or 3 mM Mg^{2+}. Spectra/Por (Spectrum Labs, Rancho Dominguez, CA) molecularporous membrane tubing with a molecular weight cutoff of 6–8

TABLE 1 Glossary of Terms

q_p	elementary charge	1.602×10^{-19} coulombs
μ	electrophoretic mobility	$cm^2/V \cdot s$
κ_D	inverse Debye length	cm^{-1}
R_s	Stokes radius	cm
$f(\kappa_D R_s)$	Henry's function	
κ	specific conductivity of buffer	mS/cm
A	cross-sectional area	cm
η	viscosity	cm^2/s
i	electric current	V/cm
λ_B	Bjerrum length	cm
$\lambda_{B\text{-aqueous}}$	Bjerrum length in water at 298 K	7.0×10^{-8} cm
D	dielectric constant	unitless
MSP	membrane scaffolding protein	
MSP1D1	MSP1D1 Nanodiscs contain ~126 lipids	−8 charge per MSP1D1
MSP1E3D1	MSP1E3D1 Nanodiscs contain ~250 lipids	−10 charge per MSP1E3D1
Z*	effective charge (valence)	$Z^* = \frac{\mu}{f_t q_p}$, unitless
ζ	zeta potential	$\zeta = \frac{3\eta}{2Df(\kappa_D R_s)}$, mV
Z_{DHH}	Debye-Hückel Henry charge (valence)	$Z_{DHH=z^*}\frac{1+\kappa R_s}{f(\kappa_D R_s)}$, unitless
Z_{calc}	charge calculated from the number of lipids in a Nanodisc	includes MSP charge contribution
$Z_{calc\cdot lipid}$	charge calculated from the number of lipids in a Nanodisc	excludes MSP charge contribution
$Z_{DHH\cdot Nanodisc}$	Nanodisc charge calculated from μ	includes MSP charge contribution
$Z_{DHH\cdot POPC}$	charge of MSP1D1 POPC Nanodisc	calculated from μ
$Z_{DHH\cdot MSP1D1}$	measured charge of MSP1D1	$Z_{DHH\cdot MSP1D1} = Z_{DHH\cdot POPC}$
$Z_{DHH\cdot Lipid}$	charge contribution from lipid only	$Z_{DHH\cdot Lipid} = Z_{DHH\cdot Nanodisc} - Z_{DHH\cdot MSP1D1}$
$Z_{DHH\cdot Fractional}$	fractional Z_{DHH}	$\frac{Z_{DHH\cdot Nanodisc}}{Z_{calculated}}$
$Z_{DHH\cdot Ca^{2+}}$	Nanodisc charge calculated from μ	In 3 mM Ca^{2+}
$Z_{DHH\cdot Mg^{2+}}$	Nanodisc charge calculated from μ	In 3 mM Mg^{2+}
$Z_{DHH\cdot Fractional}$ Ca^{2+}	fractional charge of Nanodiscs in Ca^{2+}	$\frac{Z_{DHH\cdot calcium}}{Z_{DHH\cdot Nanodisc}}$
$Z_{DHH\cdot Fractional}$ Mg^{2+}	fractional charge of Nanodiscs in Mg^{2+}	$\frac{Z_{DHH\cdot magnesium}}{Z_{DHH\cdot Nanodisc}}$
$\Delta z/\Delta PL$	Z_{DHH} contribution per unit lipid	$\frac{Z_{DHH\cdot lipid}}{\#\ of\ phospholipids}$

(lot No. 26872) was used. Membranes were prepared as described previously by Laue et al. (18). Each sample was dialyzed for another 8 h in the MCE apparatus before an experimental run. A total of three sequential runs were performed per sample. Except where noted, all measurements were made at 20°C using light intensity detection at 230 nm. Data analysis was performed according to Laue et al. (18). Stokes radius (R_s) values of ~4.7–5.1 nm for MSP1D1 Nanodiscs and ~5.7 nm for MSP1E3D1 Nanodiscs (Table S1 in the Supporting Material) were calculated from a combination of sedimentation equilibrium and sedimentation velocity data according to the method described by Cole et al. (19). These values agree with those calculated from dynamic light scattering measurements by Inagaki et al. (20). Please note that for all MCE measurements, uncertainties were obtained from N measurements, where $N \geq 9$ for each measurement.

Analytical sedimentation velocity

All Nanodisc samples were monitored at wavelengths of 280 and 230 nm with sample absorbances in the range of 0.2–0.7 OD. For POPC and POPS Nanodiscs, a fivefold dilution of the stock concentration was used. Each sample was run at a 1:5, 1:10, and 1:20 dilution at 280 and 230 nm. POPA and POPE Nanodiscs were run at their stock concentrations (1:5 and 1:10 dilutions) at 280 and 230 nm. All samples were run at 45,000 RPM, 20°C, with 150 scans acquired per analysis in a Beckman-Coulter XLA Ultracentrifuge (Brea, CA). The data were analyzed using Sedfit, SedAnal, and DC/DT+ (21–23).

Analytical sedimentation equilibrium

All Nanodisc samples were run at 15,000, 20,000, 25,000, and 30,000 RPM. Scans were acquired at 1 h intervals for 20 h per rotor speed at 20°C, using both 280 and 230 nm detection in a Beckman-Coulter XLA Ultracentrifuge. Samples were diluted to absorbances in the range of 0.2–0.7 OD at the appropriate wavelength. Before loading, each sample was dialyzed for a period of 48 h, with buffer exchange every 12 h. The data were analyzed using hetero-analysis (24).

RESULTS

Analytical electrophoresis of Nanodiscs

Nanodiscs form a single, distinct boundary in MCE that moves from the top membrane to the bottom membrane when an electric field is applied, allowing measurement of the electrophoretic mobility (μ) and subsequent calculation of the Debye-Hückel Henry charge (Z_{DHH}) from μ (Fig. 1, *A* and *B*) (15). The Nanodiscs were generally stable over a pH range from 7.0 to 8.5, a temperature range from 20.0°C to 35.0°C, and in different salt types and concentrations. With the exception of POPA Nanodiscs in Ca^{2+} and PIP_2 Nanodiscs in Mg^{2+} (Figs. S1–S3), Ca^{2+} and Mg^{2+} concentrations up to 10 mM did not cause aggregation or self-association of the Nanodiscs (Fig. S4).

POPC is a neutral lipid, but POPE is anionic

The electrophoretic mobility and Z_{DHH} values for POPC Nanodiscs presented in Table 2 include contributions from the two MSP1D1 belt proteins, whose expected charge is calculated from the amino acid composition to be −16. For POPC Nanodiscs, the total charge measured on the Nanodisc can be largely accounted for by the MSPs, with the POPC itself being neutral and thus contributing minimally to the measured charge. This observation is in general agreement with previous electrophoretic mobility measurements (25–27) showing that POPC liposomes, stearoyl-oleoylphosphatidylcholine liposomes, and egg phosphatidylcholine (PC) lipid vesicles have little to no charge. Therefore, assuming that the protein charge remains constant with the addition of lipids, and that POPC lipids contribute a net charge of zero, the MSP contribution to the Z_{DHH} of a Nanodisc can be calculated as

$$Z_{DHH\text{-}MSP1D1} = Z_{DHH\text{-}POPC} \quad (1)$$

At times, POPE is classified as a neutral lipid (28–30), owing to the anticipated cancellation of the phosphate and ammonium ion charges. However, at pH 7.4, 10POPE Nanodiscs are demonstrably more anionic than POPC Nanodiscs (Table 2; Fig. S5) and nearly as anionic as 10POPS Nanodiscs (Table 2). The observation that POPE lipids are anionic suggests that the lipid charge may play a significant role in protein-protein interactions, such as the formation of an active tissue factor:factor VIIa (TF:FVIIa) complex, in contrast to what has been assumed previously (10).

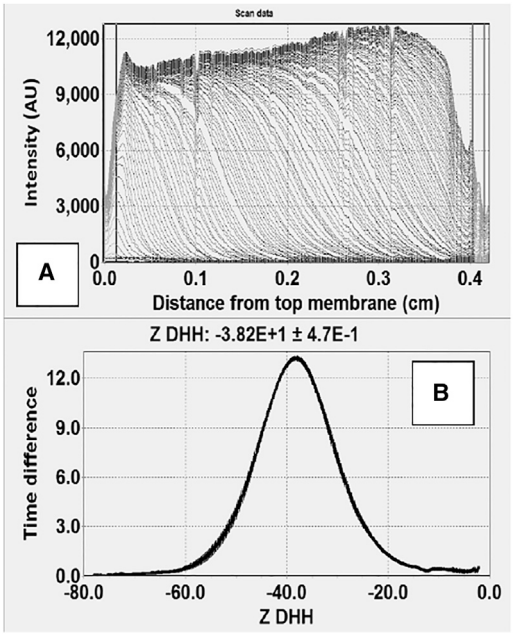

FIGURE 1 Free-boundary electrophoresis of 30POPS Nanodiscs. (*A*) Raw intensity scans show boundary movement from left to right as an intensity increase where the boundary has passed. (*B*) Distribution of Z_{DHH}.

Lipid Nanodiscs exhibit charge saturation and polyelectrolyte behavior

Highly charged macromolecules will exhibit polyelectrolyte behavior if the charged moieties are close together. The relevant parameter for polyelectrolyte behavior is the Bjerrum length, l_B (31), which is the effective distance between charge groups that yields an electrostatic potential energy

TABLE 2 Electrophoretic Mobility and Z_{DHH} of Lipid Nanodiscs

Nanodisc	μ ($cm^2/V \cdot s$)	$Z_{DHH \cdot Nanodisc}$[a]	$Z_{DHH \cdot Ca2+}$	$Z_{DHH \cdot Mg2+}$
POPC[b]	$-4.2 \times 10^{-5} \pm 3.8 \times 10^{-6}$	-14.1 ± 1.0	-10.3 ± 0.3	-14.8 ± 0.7
10% POPS[b]	$-7.1 \times 10^{-5} \pm 2.9 \times 10^{-6}$	-24.6 ± 0.8	-20.2 ± 0.4	-25.5 ± 0.8
30% POPS[b]	$-1.2 \times 10^{-4} \pm 5.7 \times 10^{-6}$	-38.5 ± 1.4	-29.5 ± 0.8	-37.9 ± 0.4
70% POPS[b]	$-1.7 \times 10^{-4} \pm 3.8 \times 10^{-6}$	-56.4 ± 2.4	-42.2 ± 1.0	-57.5 ± 1.0
POPC[b]	$-3.8 \times 10^{-5} \pm 3.9 \times 10^{-6}$	-18.0 ± 0.7	-12.6 ± 0.1	–
10% POPS[c]	$-7.9 \times 10^{-5} \pm 3.9 \times 10^{-6}$	-37.0 ± 2.0	-25.9 ± 0.1	–
30% POPS[c]	$-1.2 \times 10^{-4} \pm 3.6 \times 10^{-6}$	-57.2 ± 2.5	-39.4 ± 1.2	–
70% POPS[c]	$-2.0 \times 10^{-4} \pm 5.0 \times 10^{-6}$	-92.3 ± 4.1	-69.2 ± 4.5	–
DMPC[b]	$-4.4 \times 10^{-5} \pm 9.7 \times 10^{-7}$	-14.0 ± 0.5	–	–
10% DMPS[b]	$-6.8 \times 10^{-5} \pm 4.1 \times 10^{-6}$	-23.3 ± 0.9	–	–
30% DMPS[b]	$-1.3 \times 10^{-4} \pm 5.9 \times 10^{-6}$	-42.8 ± 0.6	–	–
50% DMPS[b]	$-1.8 \times 10^{-4} \pm 6.8 \times 10^{-6}$	-58.7 ± 1.5	–	–
10% POPA[b]	$-7.5 \times 10^{-5} \pm 1.7 \times 10^{-6}$	-26.2 ± 1.7	*	-21.1 ± 0.8
30% POPA[b]	$-1.4 \times 10^{-4} \pm 1.6 \times 10^{-5}$	-45.0 ± 3.0	*	-34.3 ± 1.6
70% POPA[b]	$-2.1 \times 10^{-4} \pm 1.0 \times 10^{-5}$	-66.6 ± 4.7	*	-45.6 ± 2.0
10% PIP_2[b]	$-1.2 \times 10^{-4} \pm 3.6 \times 10^{-6}$	-39.7 ± 1.1	-39.7 ± 1.1	*
10% POPE[b]	$-6.5 \times 10^{-5} \pm 5.3 \times 10^{-6}$	-21.4 ± 1.5	–	–
Cardiolipin[b]	$-2.4 \times 10^{-4} \pm 1.3 \times 10^{-5}$	-77.6 ± 3.6	–	–
E. coli[b]	$-1.7 \times 10^{-4} \pm 1.5 \times 10^{-6}$	-55.7 ± 0.6	*	*
E. coli[c]	$-1.7 \times 10^{-4} \pm 4.4 \times 10^{-6}$	-79.1 ± 2.0	*	*

[a]In standard solvent (100 mM NaCl, 50 mM Tris, pH 7.4). Entries without values (–) indicate that no charge measurements were made; * indicates the formation of aggregates.
[b]MSP1D1 Nanodiscs.
[c]MSP1E3D1 Nanodiscs.

that is equal in magnitude to the thermal energy (k_BT). In an aqueous system at 298 K, the Bjerrum length ($l_{B\text{-aqueous}}$) is 7.0 Å (32). In a membrane, the closest approach of lipid headgroups is on the order of $l_{B\text{-aqueous}}$ (33). Therefore, if anionic lipids are clustered on the membrane leaflet, polyelectrolyte behavior may be observed.

Because of its carboxyl group, POPS is considered to be an anionic lipid at physiological pH. As more POPS is incorporated into Nanodiscs, the magnitude of μ and Z_{DHH} increases (Tables 2 and 3), in agreement with previous observations (8,34). However, in all cases, Z_{DHH} is less than the charge calculated from the Nanodisc composition, and the discrepancy between the calculated and measured values increases with increasing phosphatidylserine (PS) content (Fig. 2). Furthermore, a calculation of the charge increment per PS shows that with increasing PS content, each additional PS contributes less to the overall charge (Table 3). This result is in accord with an increase in the effective pKa of the serine carboxyl group as the Nanodisc charge becomes more negative (1), as well as with polyelectrolyte theory, according to which a counterion (Na^+) will be bound territorially to the high potential Nanodisc surface. By themselves, our results cannot distinguish between these two possibilities.

The Nanodisc charge is insensitive to the monovalent cation and anion type

Varying the monovalent cation type did not affect μ for POPC, POPE, POPS, POPA, and PIP_2 Nanodiscs. Nearly identical values of Z_{DHH} were observed for solvents containing 100 mM Na^+, K^+, or Li^+ ions (Fig. S6). This finding differs from some previous studies in which Li^+, in particular, was reported to interact strongly with PC and PS liposomes (25,35,36). Similarly, varying the anion type had no appreciable effect on Z_{DHH} (Fig. S7).

Impact of Ca^{2+} and Mg^{2+} on the lipid Nanodisc charge

At low-micromolar concentrations, divalent cations have been shown to be important for various lipid-lipid and

TABLE 3 Z_{DHH} of the PL Component of MSP1D1 Nanodiscs

Nanodisc	$Z_{calc \cdot Lipid}$[a]	$Z_{DHH \cdot Lipid}$[b]	$Z_{DHH \cdot Lipid}/Z_{calc \cdot Lipid}$[c]	$\Delta z/\Delta PL$[d]
POPC	–	–	–	–
10POPE	−13	−7.3	0.56	−0.56
10POPS	−13	−10.5	0.81	−0.81
30POPS	−38	−24.4	0.64	−0.64
70POPS	−88	−42.3	0.48	−0.48
10POPA	−16	−12.1	0.75	−0.93
30POPA	−48	−30.9	0.64	−0.81
70POPA	−110	−52.5	0.48	−0.60
10PIP2	−39	−25.6	0.66	−2.00

[a]Calculated assuming a constant number of lipids per Nanodisc. POPS Nanodiscs were assumed to have a −1 charge per lipid, POPA Nanodiscs were assumed to have a charge of −1.25 per lipid (48), and PIP_2 Nanodiscs were assumed to have a −3 charge per lipid (51).
[b]Calculated assuming that the Z_{DHH} of POPC Nanodiscs, −14.1, is contributed entirely from the MSPs and that PC lipids contribute a Z_{DHH} of zero. Therefore, the values in the table are the measured Z_{DHH} less the MSP contribution, providing an estimate of the charge contribution solely from the lipid headgroups.
[c]Measured Z_{DHH} divided by the calculated charge.
[d]Z_{DHH} contribution per lipid headgroup ($Z_{DHH \cdot lipid}$/# of PLs).

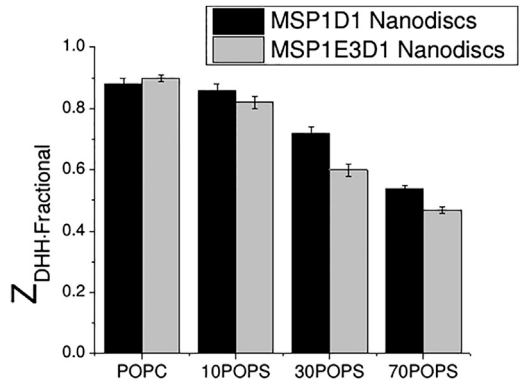

FIGURE 2 Fractional charge of MSP1D1 (*black*) and MSP1E3D1 (*gray*) Nanodiscs with varying PS content. A ratio of one means that the raw charge of the molecule is fully expressed in solution, with no neutralization from any counterions. Ratios below one mean that charge neutralization is occurring.

lipid-protein interactions (10). Ca^{2+} and Mg^{2+} are particularly relevant with respect to lipids because they are thought to affect the electrostatic properties of PLs in a manner that contributes to ion-mediated reactions with proteins, lipid translocation, and bilayer fusion/aggregation (37). Therefore, the effects of 10 μM to 10 mM Ca^{2+} and Mg^{2+} on the Nanodisc charge were determined.

The Z_{DHH} of POPC and POPS Nanodiscs was unaffected by 3 mM Mg^{2+}, whereas it decreased in the presence of 3 mM Ca^{2+} (Table 2). Curiously, even though the absolute value of the charge decrease depended on the lipid composition, the fractional charge decreased by ~25% for POPC and POPS Nanodiscs, regardless of the PS content (Fig. 3).

Even though both the POPA and PIP_2 PLs contained solvent-exposed phosphates, they exhibited different behaviors in the presence of Ca^{2+} and Mg^{2+}. The Z_{DHH} for POPA Nanodiscs was reduced by ~25% in 3 mM Mg^{2+}, but these Nanodiscs also irreversibly aggregated in the presence of 3 mM Ca^{2+} (Figs. S1 and S3). In contrast, the Z_{DHH} for PIP_2 Nanodiscs was reduced by ~50% in the presence of

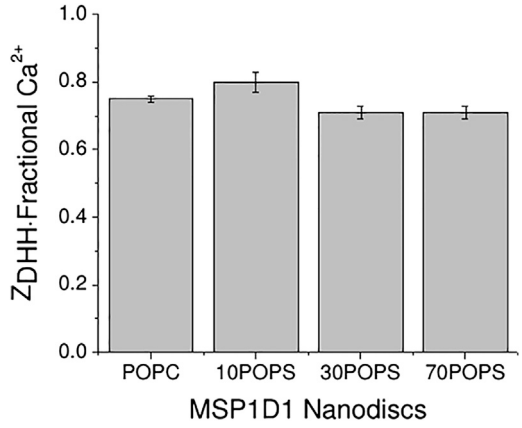

FIGURE 3 Fractional Z_{DHH} of MSP1D1 POPC and POPS Nanodiscs in the presence of 3 mM $CaCl_2$ (Table 2).

3 mM Ca^{2+}, but these Nanodiscs irreversibly aggregated in the presence of 3 mM Mg^{2+}. When POPE Nanodiscs were dialyzed (24–72 h) against solvent containing 3 mM Mg^{2+} or 3 mM Ca^{2+}, no electrophoretic boundary was formed.

DISCUSSION

General observations

Lipid Nanodiscs provide stable, uniform discoidal bilayers for biophysical studies, and MCE provides a good way to determine the molecular charge (Fig. 1). These two advances were combined to provide a survey of lipid charge and investigate the interaction of different ions with lipids. Except when irreversible Nanodisc aggregation was observed, μ and Z_{DHH} distributions were unimodal (e.g., Fig. 1 *B*), suggesting that during synthesis, different lipid types were evenly distributed among the Nanodiscs (i.e., there was no evidence for cooperative lipid incorporation by lipid type). The results presented in this work, which are believed to be both accurate and precise, will be discussed in the light of previous estimates of lipid charge and cation interactions.

MSP1D1 versus MSP1E3D1 Nanodiscs

MSP1D1 and MSP1E3D1 MSPs result in Nanodiscs that differ in size and the number of lipids per bilayer area. MSP1D1 Nanodiscs typically have a bilayer area of ~4400 Å^2 and ~126 total lipids (~63 per monolayer (38)). MSP1E3D1 Nanodiscs typically have a bilayer area of ~8900 Å^2 and ~250 total lipids (~125 per monolayer (38)). Although the absolute values of Z_{DHH} differed between MSP1D1 and MSP1E3D1 Nanodiscs (due to the increased number of lipids incorporated into the MSP1E3D1 Nanodiscs), no significant differences were observed between the Z_{DHH} values of MSP1D1 and MSP1E3D1 Nanodiscs with respect to the different solvent conditions used, such as the monovalent alkali cation type and temperature. Therefore, it was assumed that any effects seen with MSP1D1 Nanodiscs would also be observed with MSP1E3D1 Nanodiscs.

PL phase transition temperature

Temperature differences can have a wide variety of effects on lipid microenvironments depending on the lipid components that are present. For example, the phase transition temperature of different lipids can vary depending on which fatty acids are present, which in turn affects the fluidity of the lipid bilayer (39). POPA lipids, in particular, have a phase transition temperature of ~28°C, whereas POPC and POPS lipids have phase transition temperatures of ~−2°C and ~14°C, respectively. For dimyristoylphosphatidylcholine (DMPC) lipids, the phase transition temperature is ~24°C, and for 1,2-dimyristoyl-sn-glycero-3-phospho-L-serine (DMPS)

Nanodiscs the phase transition temperature is ~35°C. Temperature experiments were performed at 15°C, 20°C, 25°C, and 35°C. It was observed that when the viscosity and conductivity changes were accounted for, Z_{DHH} did not change significantly for all Nanodiscs, regardless of the lipid and fatty-acid contents (Table S2; Figs. S8 and S9). Therefore, although the temperature may affect the packing of the PLs within the discoidal bilayer, it does not affect the overall charge.

Polyelectrolyte behavior of lipid Nanodiscs

One characteristic of a polyelectrolyte is that extrapolation of the charge to zero salt will result in a value that is less than what would be expected on the basis of the composition. The extent of the discrepancy between expectation and measurement depends on the shape of the polyelectrolyte, since planar structures are expected to result in a greater discrepancy (31). To test the polyelectrolyte nature of lipid Nanodiscs, charge measurements were obtained as a function of salt concentration (Fig. S10; Table S3) and the resulting data were fit to a third-order polynomial to estimate the charge at zero salt. As can be seen in Fig. S10, the neutral POPC Nanodiscs exhibit relatively little salt dependence, with the extent of the salt dependence increasing as the Nanodisc composition includes more anionic lipids. Furthermore, there is a concomitant discrepancy in the extrapolated values of Z_{DHH} with the more highly charged Nanodiscs. These results not only affirm the polyelectrolyte nature of lipid Nanodiscs but also suggest that membrane microdomains (lipid rafts) may provide regions that exhibit polyelectrolyte behavior. Such regions would have different divalent cation interactions and, potentially, different protein-lipid interactions.

Using POPC as a neutral lipid standard

POPC Nanodiscs were observed to have an electrophoretic mobility of $-4.2 \times 10^{-5} \pm 3.8 \times 10^{-6}$ $cm^2/V \cdot s$, resulting in a Z_{DHH} of -14.1 ± 1.0 (Table 2). This value of Z_{DHH} differs by +1.9 charge units from the charge calculated from the amino acid composition of two MSP1D1 proteins alone. The uncertainty in Z_{DHH} from MCE measurements is estimated to be ±6% (9,40), or ±0.8 charge units for POPC Nanodiscs. Although it is difficult to estimate the uncertainty in the charge calculated from the amino acid composition, it is almost certainly greater than 6% (15). Even if the calculated MSP1D1 charge was accurate, the resulting POPC charge would be near neutral (+0.06/lipid, calculated as +1.9 per 63 lipid molecules). Similar conclusions were reached with the MSP1E3D1 Nanodiscs (Table 2), reinforcing the conclusion that POPC is neutral. For the remainder of this discussion, it is assumed that the MSP1D1 protein charge contribution to the Z_{DHH} of Nanodiscs is −14.1. At present, we cannot say that the MSP charge is independent of the lipid composition. However, if this implicit assumption is made, the charge on the MSP1D1 component of Nanodiscs may be estimated as shown in Eq. 1.

Our results for POPC generally agree with previous work indicating that POPC is neutral (25–28). The observation that the POPC Nanodisc charge was unaffected by the monovalent alkali cation type (Fig. S6) is consistent with infrared spectroscopy studies that showed little effect of monovalent cations on the absorption bands of phosphate carbonyl groups, and attributed the small changes that were observed to solvation differences (41). Likewise, NMR spectroscopy revealed that neither K^+ nor Na^+ significantly perturbed PC liposome spectra (42), and estimates of the binding constants for Na^+ (0.15 M^{-1}), K^+ (0.15 M^{-1}), and Li^+ (0.3 M^{-1}) to PC lipids were significantly less than those determined for Mg^{2+} (~30 M^{-1}) and Ca^{2+} (~40 M^{-1}) (43). Our data also are consistent with previous observations made using electrophoretic methods (41,42), with the exception of the results obtained by Klasczyk et al. (25) using electrophoretic light scattering (ELS) and POPC vesicles. Their data show vastly different electrophoretic mobilities in the presence of Li^+, K^+, and Na^+ ions. However, in general, ELS charge measurements for macromolecules the size of Nanodiscs have poor precision (15), which is evident in the ELS mobility data for PC vesicles, where the uncertainty nearly equals or exceeds the reported mobility (25).

POPE is an anionic lipid

In 100 mM NaCl, 50 mM Tris, pH 7.4, 10POPE Nanodiscs have an electrophoretic mobility of $-6.5 \times 10^{-5} \pm 5.3 \times 10^{-6}$ $cm^2/V \cdot s$ (Table 2), resulting in a Z_{DHH} of -21.4 ± 1.5, which is considerably more anionic than POPC Nanodiscs (-14.1 ± 1.0) and only slightly less anionic than 10POPS Nanodiscs (-24.6 ± 0.8). Taking the MSP charge contribution into account, it was calculated that the Z_{DHH} contribution per lipid of 10POPE lipids is ~−0.5 charge units in standard buffer.

The anionic nature of 10POPE Nanodiscs demonstrated herein is inconsistent with some earlier reports that phosphatidylethanolamine (PE) is a neutral lipid. Roy et al. (8) observed that 10% PE liposomes in 1 mM phosphate, 1 mM NaCl, pH 7.4, have a ζ potential that is 7 mV more anionic than that of PC liposomes, whereas 10% PS liposomes in the same solvent are ~30 mV more anionic. Based on these results, they concluded that the PE charge was more similar to the PC charge than to that of PS. Using similar methods, comparable conclusions were reached by Davidson et al. (44) in 150 mM NaCl, 10 mM Tris, pH 8.6, and by Woodle et al. (45) in 10 mM phosphate buffer, pH 7.3.

Nonelectrophoretic evidence, however, is consistent with PE behaving similarly to anionic lipids. For example, factor X (FX) activation by TF:FVIIa requires anionic lipids, particularly PS (46). Previous studies showed that incorporation of other anionic lipids (such as phosphatidic acids, phosphatidylglycerol, and phosphatidylinositol) decreases

the PS requirement for FX activation, whereas PC does not (10). In those studies, PE lipids were also found to reduce the PS requirement nearly as well as phosphatidic acids, phosphatidylglycerol, and phosphatidylinositol, consistent with the lipid charge being an important contributor to the FX-lipid interaction. Likewise, it was shown that spectrin binds to PE/PC lipid vesicles nearly as well as it does to PS/PC vesicles (47). In both of these cases, the data were interpreted as though PE were neutral, leading to the conclusion that only structural, and not charge, features are important for the interaction. Although structural considerations are important, our results show that charge considerations should not be overlooked. In general, our findings suggest that earlier conclusions based on PE being a neutral lipid must be reconsidered.

The ammonium headgroup of PE is titratable, with the pKa of an isolated PE headgroup being estimated to be 11.25 (48). However, in the context of the bilayer, a POPE will be in the vicinity of other cationic PE headgroups, which will lower the effective pKa (1). For this reason, the Z_{DHH} for POPA, POPE, POPS, POPC, and PIP_2 was measured at pH 7.0, 7.5, 8.0, and 8.5 (Figs. S11 and S12).

POPS

POPS Nanodiscs were observed to be more anionic than POPC and POPE Nanodiscs (Table 2), which agrees qualitatively with previous observations (8,34,37). Likewise, our observation that the monovalent cation type has little effect on Nanodisc charge (Fig. S6) is in agreement with a previous study by Eisenberg et al. (39), in which the ζ potentials of PS lipids in the presence of Na^+, Li^+, and K^+ did not differ significantly. Similarly, isothermal titration data show that the binding constants for Na^+ and K^+ to liposomes are on the order of 0.15–0.44 M^{-1} (49). Our results disagree with the x-ray diffraction data of Loosley-Millman et al. (35) and with the NMR results of Srinivasan et al. (36), who reported that in unbuffered organic solvents, Li^+ interacts with anionic lipids, and specifically with PS.

POPA Nanodiscs have a higher charge than POPS Nanodiscs containing similar lipid contents at pH 7.4

It has been suggested that both PS and PA lipids have a net charge of -1 at physiologic pH (50). However, the phosphate on PA has a pKa (~8.0) within the physiologic range and potentially can exhibit a net charge of -1 to -2 depending on the local lipid microenvironment. Titration data reported by Marsh (48) suggest that the charge on PA lipids is closer to -1.25 at pH 7.4, in accordance with our data (Tables 2 and 3).

The electrophoretic mobility and Z_{DHH} values for POPA Nanodiscs in Table 2 qualitatively agree with electrophoretic measurements made by Piret et al. (50) in 40 mM citrate, 40 mM phosphate, pH 5.4, which showed that the μ of 10% PA lipid vesicles is similar (but not identical) to that of 10% PS lipid vesicles. However, our data differ quantitatively from those of Piret et al. because we used different solvent conditions, particularly with regard to pH, and it is not surprising that the charge is greater at pH 7.4 than at pH 5.4.

To our knowledge, there are no previous electrophoretic data on the effects of different monovalent alkali cations on PA-containing lipids. However, the charge data reported here generally agree with the x-ray diffraction data of Loosely-Millman et al. (35), which show that POPA interacts with Na^+, K^+, and Li^+ similarly.

PIP_2

PIP_2 Nanodiscs have an electrophoretic mobility of $-1.2 \times 10^{-4} \pm 3.6 \times 10^{-6}$ $cm^2/V \cdot s$, yielding a Z_{DHH} of -39.7 ± 1.1 (Table 2). This suggests that the headgroup of PIP_2 carries a -3 charge, and is supported by the fact that 10PIP_2 Nanodiscs exhibit a charge similar to that of 30POPS Nanodiscs (-38.5 ± 1.4). Toner et al. (51) found that the ζ potential of PIP_2 lipid vesicles was three times greater than that of PI lipid vesicles, which also is consistent with a -3 charge per headgroup.

Interactions of lipid Nanodiscs with Ca^{2+} and Mg^{2+}

Divalent cations, particularly Ca^{2+} and Mg^{2+}, have been shown to be important for a variety of lipid-protein interactions (10,52). Consequently, the effect of physiological concentrations of these divalent cations on the lipid Nanodisc charge was determined. The interaction of POPC and POPS Nanodiscs in 100 mM NaCl, 50 mM Tris, 3 mM $CaCl_2$, pH 7.4, resulted in an ~25% decrease in Z_{DHH} compared with solvent lacking Ca^{2+} (Fig. 3). In contrast, similar concentrations of Mg^{2+} had little effect on the Z_{DHH} of POPC and POPS Nanodiscs over the concentration range of 10 μM to 10 mM (Fig. S5). It is possible that the differences between Ca^{2+} and Mg^{2+} interactions with these two lipids may account for some of the differences in their supporting protein interactions with these lipids (52).

The addition of 3 mM Ca^{2+} resulted in a nearly identical *fractional* charge change, but different *absolute* charge change, for POPC and POPS Nanodiscs (Fig. 3). This observation is inconsistent with a model in which Ca^{2+} interacts solely with MSPs. Instead, these results are consistent with a model in which there is a difference in preferential solvation of the Nanodiscs by 3 mM Ca^{2+} compared with 100 mM Na^+, and suggests that Ca^{2+} does not have a specific interaction with PC or PS headgroups, contrary to some other models (42). However, the data do not specifically rule out the possibility that PS provides a Ca^{2+}-specific binding site. It may seem somewhat surprising that pure POPC Nanodiscs interact with Ca^{2+}; however, this interaction appears to be weak, and may involve either the lipid or protein portion of the Nanodiscs (4). Perhaps more surprising is the observation that Ca^{2+} neutralized the same fraction of the

expected charge regardless of the PS content (Fig. 3), which we cannot explain at this time.

Our results do not agree with previous findings from NMR studies of POPC liposomes that were collected at much higher Ca^{2+} concentrations, which were interpreted as showing a stronger, more specific interaction of Ca^{2+} with POPC (42). Also, our results disagree with stability and binding studies (53–55) that suggested that specific binding occurs between Ca^{2+} and the phosphate portion of the PL. Perhaps the relative instability and heterogeneity (in size and possibly composition) of the liposome preparations and the different solvent conditions used (specifically the Ca^{2+} concentrations) contribute to these differences. In addition, many NMR studies that investigated Ca^{2+} interactions with lipids assumed that 1) one Ca^{2+} ion binds two lipids, 2) any shifts in signal are solely due to the Ca^{2+} ion, and 3) the binding affinities of zwitterionic and anionic PLs are identical (56). Electrophoresis does not make these assumptions, and Z_{DHH} is calculated directly from μ. However, electrophoresis cannot distinguish between specific ion binding and adsorption due to preferential solvation effects.

The addition of 3 mM Mg^{2+} did not significantly affect the electrophoretic mobility and Z_{DHH} values of POPC and POPS Nanodiscs (Table 2). Martín-Molina et al. (37) reported that in 100 mM $NaNO_3$, pH 5.4, increasing [Mg^{2+}] decreased the magnitude of μ for both PC and PS liposomes, with a charge inversion (sign reversal) occurring at 100 mM Mg^{2+}. There is no reason to suspect that the nitrate ion would account for the difference between their data and ours, since the anion type appears to have little effect on the lipid charge (Fig. S7). Perhaps the discrepancy is a consequence of the much higher [Mg^{2+}] used in their studies.

POPA

In the presence of 3 mM Ca^{2+}, POPA Nanodiscs aggregated irreversibly to form highly anionic clusters (Figs. S1 and S3), which is in general agreement with previous studies on Ca^{2+}-induced POPA aggregation (57). However, the fact that the POPA aggregates remained anionic suggests that neutralization of the surface charge may not underlie the aggregation phenomenon, as was suggested previously (58). Instead, our data are consistent with a model in which Ca^{2+} bridges Nanodiscs. At 10 μM [Ca^{2+}], no aggregation was observed and the Z_{DHH} was similar to that of POPA Nanodiscs in the absence of Ca^{2+}, suggesting that tight ion binding was not occurring.

As shown in Fig. 4, the fractional Z_{DHH} of POPA Nanodiscs in the presence of 3 mM Mg^{2+} is similar to the fractional Z_{DHH} of POPS Nanodiscs in the presence of 3 mM Ca^{2+}. This suggests that there may be an underlying mechanism similar to that employed in the charge reduction, such as preferential solvation. With respect to POPA behavior in the presence of Mg^{2+}, data in the literature (albeit limited) regarding Mg^{2+}/POPA interactions suggest that Mg^{2+} induces aggregation (59). We did not observe Mg^{2+}-induced aggregation (Fig. S1) of POPA Nanodiscs, although an interaction is implied by the reduced magnitude of Z_{DHH}. It has been observed that the presence of Mg^{2+} typically does not lead to bilayer fusion, but does lead to aggregation (60). Therefore, the interaction between Mg^{2+} and POPA appears to be fundamentally different from that between Ca^{2+} and POPA, since Ca^{2+} induced aggregation of POPA Nanodiscs, but Mg^{2+} did not. MCE mobility measurements show that POPA Nanodiscs remained monodisperse in the presence of 3 mM Mg^{2+} (Fig. S1). The interaction with Mg^{2+} must involve the exposed phosphate group on PA lipids and not the MSPs, since Mg^{2+} did not have an effect on POPC and POPS Nanodiscs, which also contain MSPs. Furthermore, the data suggest that Mg^{2+} also does not have a significant interaction with the carboxylate anion on the PS lipid headgroup, as the electrophoretic mobility of POPS Nanodiscs was not significantly different in the presence of Mg^{2+}. However, Mg^{2+} does bind with phosphate ions, which suggests that the phospho-L-serine moiety of the PS lipid headgroup may prevent Mg^{2+} from interacting with the phospho moiety in PS lipids in a manner similar to that observed for the bulky phospho-L-choline headgroup of PC lipids.

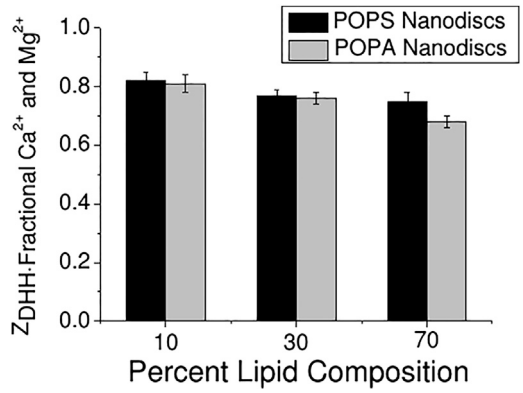

FIGURE 4 Comparison of the fractional Z_{DHH} between POPS Nanodiscs in the presence of 3 mM Ca^{2+} (*black*) and POPA Nanodiscs in the presence of Mg^{2+} (*gray*).

PIP_2 Nanodiscs aggregate in the presence of Mg^{2+}, but not Ca^{2+}

PIP_2 Nanodiscs, like POPA Nanodiscs, were observed to interact with both Ca^{2+} and Mg^{2+} (Fig. S2). However, the nature of these interactions was the opposite of that observed with POPA Nanodiscs, in that PIP_2 Nanodiscs aggregated irreversibly in the presence of Mg^{2+} but remained monodisperse in Ca^{2+}. The Z_{DHH} of PIP_2 Nanodiscs decreased in magnitude in the presence of Ca^{2+}. Furthermore, the charge neutralization by Ca^{2+} was of a much greater magnitude than that observed for all other Nanodiscs (~25% for POPC and POPS versus ~50% for PIP_2; Table 2; Fig. 5).

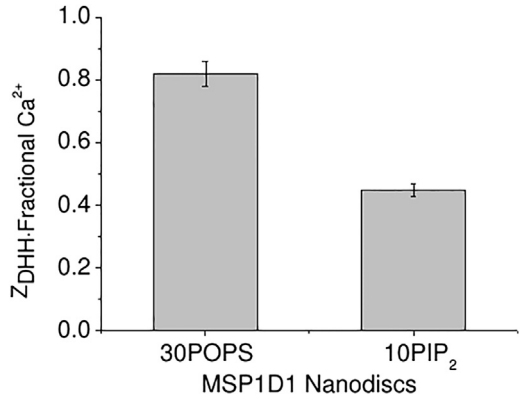

FIGURE 5 Comparison of the fractional Z_{DHH} of 30POPS Nanodiscs and 10PIP$_2$ Nanodiscs in the presence of 3 mM Ca^{2+}.

Other studies also have shown that PIP$_2$ Nanodiscs bind Ca^{2+} and Mg^{2+} differently (61), but they conflict in that some report that PIP$_2$ lipids bind Ca^{2+} more strongly and others report that PIP$_2$ lipids bind Mg^{2+} more strongly (61,62). For example, Ca^{2+} has been observed to induce stronger aggregation behavior than Mg^{2+} (57,61); however, we did not observe Ca^{2+}-induced aggregation with PIP$_2$ Nanodiscs.

CONCLUSION

In this work, we quantitated the precise charge on various lipid types as they exist in a soluble membrane bilayer. Such information is critical if one is to understand the role of lipid charge in mediating the interaction of proteins with membrane surfaces. Such interactions play critical roles in important biological processes, including signaling by K-Ras4b and integrins, and the initiation of blood coagulation.

SUPPORTING MATERIAL

Fourteen figures and three tables are available at http://www.biophysj.org/biophysj/supplemental/S0006-3495(16)30527-6.

ACKNOWLEDGMENTS

The research at the University of Montana was performed in the Biospectroscopy Core Research Laboratory, which is supported by National Institutes of Health CoBRE award P20GM103546 to the Center for Biomolecular Structure and Dynamics. The research at the University of New Hampshire was supported by the Biomolecular Interaction Technologies Center and the Center to Advance Molecular Interaction Science. The research at the University of Illinois at Urbana-Champaign was supported by the National Institutes of Health (GM118145 and GM111048).

REFERENCES

1. Edsall, J. T., and J. Wyman. 1958. Biophysical Chemistry, Vol. I: Thermodynamics, Electrostatics, and the Biological Significance of the Properties of Matter. Academic Press, New York.
2. O'Brien, R. W., and L. R. White. 1978. Electrophoretic mobility of a spherical colloidal particle. *J. Chem. Soc., Faraday Trans. II.* 74:1607–1626.
3. Scatchard, G., and E. S. Black. 1949. The effect of salts on the isoionic and isoelectric points of proteins. *J. Phys. Colloid Chem.* 53:88–99.
4. Gokarn, Y. R., R. M. Fesinmeyer, …, D. N. Brems. 2011. Effective charge measurements reveal selective and preferential accumulation of anions, but not cations, at the protein surface in dilute salt solutions. *Protein Sci.* 20:580–587.
5. Hayes, D. B. 1993. Equilibrium electrophoresis: results from the second prototype. PhD thesis. University of New Hampshire, Durham, NH.
6. Wooll, J. 1996. Investigation of $Pd(A)_{20}$ $Pd(T)_{20}$ in the analytical electrophoresis apparatus. PhD dissertation. University of New Hampshire, Durham, NH.
7. May, C. 2007. Valence and structure relationships in oligonucleotides. PhD dissertation. University of New Hampshire, Durham, NH.
8. Roy, M. T., M. Gallardo, and J. Estelrich. 1998. Influence of size on electrokinetic behavior of phosphatidylserine and phosphatidylethanolamine lipid vesicles. *J. Colloid Interface Sci.* 206:512–517.
9. Durant, J. 2003. Free solution electrophoresis measurements and their theoretical relationships to net protein valence. PhD dissertation. University of New Hampshire, Durham, NH.
10. Tavoosi, N., R. L. Davis-Harrison, …, J. H. Morrissey. 2011. Molecular determinants of phospholipid synergy in blood clotting. *J. Biol. Chem.* 286:23247–23253.
11. Heiger, D. N. 1992. High Performance Capillary Electrophoresis: An Introduction. Hewlett-Packard, Böblingen, Germany.
12. Bayburt, T. H., and S. G. Sligar. 2010. Membrane protein assembly into Nanodiscs. *FEBS Lett.* 584:1721–1727.
13. Nath, A., W. M. Atkins, and S. G. Sligar. 2007. Applications of phospholipid bilayer nanodiscs in the study of membranes and membrane proteins. *Biochemistry.* 46:2059–2069.
14. Ridgeway, T. M., D. B. Hayes, …, T. M. Laue. 1998. An apparatus for membrane-confined analytical electrophoresis. *Electrophoresis.* 19:1611–1619.
15. Filoti, D. I., S. J. Shire, …, T. M. Laue. 2015. Comparative study of analytical techniques for determining protein charge. *J. Pharm. Sci.* 104:2123–2131.
16. Saiz, L., and M. L. Klein. 2002. Electrostatic interactions in a neutral model phospholipid bilayer by molecular dynamics simulations. *J. Chem. Phys.* 116:3052–3057.
17. Gurtovenko, A. A., and I. Vattulainen. 2008. Effect of NaCl and KCl on phosphatidylcholine and phosphatidylethanolamine lipid membranes: insight from atomic-scale simulations for understanding salt-induced effects in the plasma membrane. *J. Phys. Chem. B.* 112:1953–1962.
18. Laue, T. M., A. L. Hazard, …, D. A. Yphantis. 1989. Direct determination of macromolecular charge by equilibrium electrophoresis. *Anal. Biochem.* 182:377–382.
19. Cole, J. L., J. W. Lary, T. Moody, and T. M. Laue. 2008. Analytical ultracentrifugation: sedimentation velocity and sedimentation equilibrium. *Methods Cell Biol.* 84:143–179.
20. Inagaki, S., R. Ghirlando, and R. Grisshammer. 2013. Biophysical characterization of membrane proteins in nanodiscs. *Methods.* 59:287–300.
21. Schuck, P. 2000. Size-distribution analysis of macromolecules by sedimentation velocity ultracentrifugation and Lamm equation modeling. *Biophys. J.* 78:1606–1619.
22. Stafford, W. 2003. Analytical ultracentrifugation: sedimentation velocity analysis. *Curr. Protoc. Protein Sci.* Chapter 20, Unit 20.7.
23. Philo, J. S. 2000. A method for directly fitting the time derivative of sedimentation velocity data and an alternative algorithm for calculating sedimentation coefficient distribution functions. *Anal. Biochem.* 279:151–163.

24. Cole, J. L., and J. C. Hansen. 1999. Analytical ultracentrifugation as a contemporary biomolecular research tool. *J. Biomol. Tech.* 10:163–176.

25. Klasczyk, B., V. Knecht, …, R. Dimova. 2010. Interactions of alkali metal chlorides with phosphatidylcholine vesicles. *Langmuir.* 26:18951–18958.

26. McLaughlin, A., C. Grathwohl, and S. McLaughlin. 1978. The adsorption of divalent cations to phosphatidylcholine bilayer membranes. *Biochim. Biophys. Acta.* 513:338–357.

27. Pincet, F., S. Cribier, and E. Perez. 1999. Bilayers of neutral lipids bear a small but significant charge. *Eur. Phys. J. B.* 11:127–130.

28. Gunstone, F. D., J. L. Harwood, and F. B. Padley. 1994. The Lipid Handbook, 2nd ed. Chapman and Hall, London.

29. Murzyn, K., T. Róg, and M. Pasenkiewicz-Gierula. 2005. Phosphatidylethanolamine-phosphatidylglycerol bilayer as a model of the inner bacterial membrane. *Biophys. J.* 88:1091–1103.

30. Istokovics, A., N. Morita, …, H. Okuyama. 1998. Neutral lipids, phospholipids, and a betaine lipid of the snow mold fungus Microdochium nivale. *Can. J. Microbiol.* 44:1051–1059.

31. Manning, G. S. 1969. Limiting laws and counterion condensation in polyelectrolyte solutions I. Colligative properties. *J. Chem. Phys.* 51:924–933.

32. Morfin, I., F. Horkay, …, E. Geissler. 2004. Adsorption of divalent cations on DNA. *Biophys. J.* 87:2897–2904.

33. Levental, I., P. A. Janmey, and A. Cēbers. 2008. Electrostatic contribution to the surface pressure of charged monolayers containing polyphosphoinositides. *Biophys. J.* 95:1199–1205.

34. Kato, K., M. Koido, …, T. Ichiki. 2011. Precise evaluation of electrophoretic mobility distribution of nanoliposomes using microcapillary electrophoresis ships with sensitive fluorescent imaging. School of Engineering, University of Tokyo, Tokyo.

35. Loosley-Millman, M. E., R. P. Rand, and V. A. Parsegian. 1982. Effects of monovalent ion binding and screening on measured electrostatic forces between charged phospholipid bilayers. *Biophys. J.* 40:221–232.

36. Srinivasan, C., N. Minadeo, …, D. Mota de Freitas. 1999. Competition between Li+ and Mg2+ for red blood cell membrane phospholipids: a 31P, 7Li, and 6Li nuclear magnetic resonance study. *Lipids.* 34:1211–1221.

37. Martín-Molina, A., C. Rodríguez-Beas, and J. Faraudo. 2012. Effect of calcium and magnesium on phosphatidylserine membranes: experiments and all-atomic simulations. *Biophys. J.* 102:2095–2103.

38. Ritchie, T. K., Y. V. Grinkova, …, S. G. Sligar. 2009. Chapter 11—Reconstitution of membrane proteins in phospholipid bilayer nanodiscs. *Methods Enzymol.* 464:211–231.

39. Eisenberg, M., T. Gresalfi, …, S. McLaughlin. 1979. Adsorption of monovalent cations to bilayer membranes containing negative phospholipids. *Biochemistry.* 18:5213–5223.

40. Jordon, K. 2014. Real-time electrophoretic mobility in membrane confined electrophoresis. Master's thesis. University of New Hampshire, Durham, NH.

41. Binder, H., and O. Zschörnig. 2002. The effect of metal cations on the phase behavior and hydration characteristics of phospholipid membranes. *Chem. Phys. Lipids.* 115:39–61.

42. Altenbach, C., and J. Seelig. 1984. Ca^{2+} binding to phosphatidylcholine bilayers as studied by deuterium magnetic resonance. Evidence for the formation of a Ca^{2+} complex with two phospholipid molecules. *Biochemistry.* 23:3913–3920.

43. Tatulian, S. A. 1987. Binding of alkaline-earth metal cations and some anions to phosphatidylcholine liposomes. *Eur. J. Biochem.* 170:413–420.

44. Davidson, W. S., D. L. Sparks, …, M. C. Phillips. 1994. The molecular basis for the difference in charge between pre-β- and α-migrating high density lipoproteins. *J. Biol. Chem.* 269:8959–8965.

45. Woodle, M. C., L. R. Collins, …, F. J. Martin. 1992. Sterically stabilized liposomes. Reduction in electrophoretic mobility but not electrostatic surface potential. *Biophys. J.* 61:902–910.

46. Heemskerk, J. W. M., E. M. Bevers, and T. Lindhout. 2002. Platelet activation and blood coagulation. *Thromb. Haemost.* 88:186–193.

47. O'Toole, P. J., I. E. Morrison, and R. J. Cherry. 2000. Investigations of spectrin-lipid interactions using fluoresceinphosphatidylethanolamine as a membrane probe. *Biochim. Biophys. Acta.* 1466:39–46.

48. Marsh, D. 1990. Handbook of Lipid Bilayers, 2nd ed. CRC Press, Boca Raton, FL.

49. Knecht, V., and B. Klasczyk. 2013. Specific binding of chloride ions to lipid vesicles and implications at molecular scale. *Biophys. J.* 104:818–824.

50. Piret, J., A. Schanck, …, M. P. Mingeot-Leclercq. 2005. Modulation of the in vitro activity of lysosomal phospholipase A1 by membrane lipids. *Chem. Phys. Lipids.* 133:1–15.

51. Toner, M., G. Vaio, …, S. McLaughlin. 1988. Adsorption of cations to phosphatidylinositol 4,5-bisphosphate. *Biochemistry.* 27:7435–7443.

52. Bulkin, B. J., and R. Hauser. 1973. Lipid-protein interactions: role of divalent ions in binding of glycylglycine to phosphatidylserine. *Biochim. Biophys. Acta.* 326:289–292.

53. Ekerdt, R., and D. Papahadjopoulos. 1982. Intermembrane contact affects calcium binding to phospholipid vesicles. *Proc. Natl. Acad. Sci. USA.* 79:2273–2277.

54. Nir, S., N. Düzgüneş, and J. Bentz. 1983. Binding of monovalent cations to phosphatidylserine and modulation of Ca^{2+}- and Mg^{2+}-induced vesicle fusion. *Biochim. Biophys. Acta.* 735:160–172.

55. Roux, M., and M. Bloom. 1990. Ca^{2+}, Mg^{2+}, Li^{+}, Na^{+}, and K^{+} distributions in the headgroup region of binary membranes of phosphatidylcholine and phosphatidylserine as seen by deuterium NMR. *Biochemistry.* 29:7077–7089.

56. Huster, D., K. Arnold, and K. Gawrisch. 2000. Strength of Ca(2+) binding to retinal lipid membranes: consequences for lipid organization. *Biophys. J.* 78:3011–3018.

57. Serhan, C. N., M. J. Broekman, …, G. Weissmann. 1983. Changes in phosphatidylinositol and phosphatidic acid in stimulated human neutrophils. Relationship to calcium mobilization, aggregation and superoxide radical generation. *Biochim. Biophys. Acta.* 762:420–428.

58. Papahadjopoulos, D., S. Nir, and N. Düzgünes. 1990. Molecular mechanisms of calcium-induced membrane fusion. *J. Bioenerg. Biomembr.* 22:157–179.

59. Leventis, R., J. Gagné, …, J. R. Silvius. 1986. Divalent cation induced fusion and lipid lateral segregation in phosphatidylcholine-phosphatidic acid vesicles. *Biochemistry.* 25:6978–6987.

60. Schultz, Z. D., I. M. Pazos, …, I. W. Levin. 2009. Magnesium-induced lipid bilayer microdomain reorganizations: implications for membrane fusion. *J. Phys. Chem. B.* 113:9932–9941.

61. Wang, Y. H., A. Collins, …, P. A. Janmey. 2012. Divalent cation-induced cluster formation by polyphosphoinositides in model membranes. *J. Am. Chem. Soc.* 134:3387–3395.

62. Granyanya, A., K. R. Sipido, …, K. Mubagwa. 2006. ATP and PIP2 dependence of the magnesium-inhibited, TRM7-like cation channel in cardiac myocytes. *Am. J. Physiol.* 291:C627–C635.

Biophysical Journal, Volume *111*

Supplemental Information

The Charge Properties of Phospholipid Nanodiscs

Cheng Her, Dana I. Filoti, Mark A. McLean, Stephen G. Sligar, J.B. Alexander Ross, Harmen Steele, and Thomas M. Laue

THE CHARGE PROPERTIES OF PHOSPHOLIPID NANODISCS

Cheng Her,* Dana I. Filoti,* Mark A. McLean,† Stephen G. Sligar,†, J.B. Alexander Ross‡, Harmen Steele‡ and Thomas M. Laue*

*Department of Molecular, Cellular and Biomedical Sciences, University of New Hampshire, Durham NH, USA; †Department of Biochemistry, University of Illinois at Urbana-Champaign, Champaign IL, US; ‡Department of Chemistry and Biochemistry, University of Montana, Missoula MT, USA

Supporting Materials

Table S1
Hydrodynamic properties of lipid Nanodiscs

Nanodisc	M_b (kDa)	$S_{20,w}$ [a]	R_s (nm)	$\bar{\upsilon}$ (cm^3/g)
MSP1D1 POPC	14.3 ± 0.4	$3.0_{52} \pm 5.0 \times 10^{-3}$	$4.7 \pm 5.0 \times 10^{-2}$	$0.88_8 \pm 3.0 \times 10^{-3}$
MSP1D1 10% POPS	15.5 ± 0.4	$3.1_{27} \pm 5.0 \times 10^{-3}$	$4.9 \pm 3.0 \times 10^{-2}$	$0.89_2 \pm 4.0 \times 10^{-3}$
MSP1D1 30% POPS	17.8 ± 0.6	$3.5_{09} \pm 3.0 \times 10^{-3}$	$5.0 \pm 5.0 \times 10^{-2}$	$0.87_9 \pm 4.0 \times 10^{-3}$
MSP1D1 70% POPS	21.6 ± 0.7	$4.4_{27} \pm 5.0 \times 10^{-3}$	$4.8 \pm 4.0 \times 10^{-2}$	$0.88_6 \pm 3.0 \times 10^{-3}$
MSP1E3D1 POPC	16.8 ± 1.2	$2.9_{37} \pm 4.0 \times 10^{-3}$	$5.7 \pm 8.0 \times 10^{-2}$	$0.89_9 \pm 3.0 \times 10^{-3}$
MSP1E3D1 10% POPS	19.0 ± 0.6	$3.2_{59} \pm 2.0 \times 10^{-3}$	$5.8 \pm 1.0 \times 10^{-1}$	$0.88_9 \pm 2.0 \times 10^{-2}$
MSP1E3D1 30% POPS	20.6 ± 0.6	$3.6_{21} \pm 4.0 \times 10^{-3}$	$5.7 \pm 6.0 \times 10^{-2}$	$0.89_1 \pm 4.0 \times 10^{-3}$
MSP1E3D1 70% POPS	26.7 ± 1.1	$4.6_{41} \pm 3.0 \times 10^{-3}$	$5.7 \pm 1.0 \times 10^{-1}$	$0.88_9 \pm 3.0 \times 10^{-3}$
MSP1D1 10% POPA	14.6 ± 0.8	$3.0_{22} \pm 3.0 \times 10^{-3}$	$4.8 \pm 6.0 \times 10^{-2}$	$0.89_1 \pm 4.0 \times 10^{-3}$
MSP1D1 30% POPA	15.7 ± 0.8	$3.1_{76} \pm 6.0 \times 10^{-3}$	$4.9 \pm 6.0 \times 10^{-2}$	$0.88_9 \pm 4.0 \times 10^{-3}$
MSP1D1 70% POPA	18.5 ± 1.0	$3.5_{95} \pm 8.0 \times 10^{-3}$	$5.1 \pm 1.1 \times 10^{-1}$	$0.88_9 \pm 3.0 \times 10^{-3}$
MSP1D1 10% POPE	14.6 ± 0.6	$3.0_{31} \pm 4.0 \times 10^{-3}$	$4.8 \pm 4.0 \times 10^{-2}$	$0.88_9 \pm 2.0 \times 10^{-3}$
MSP1D1 10% PIP_2	-	-	-	-
MSP1D1 Cardiolipin	-	-	-	-
MSP1D1 *E. coli* [b]	-	$3.2_{87} \pm 5.0 \times 10^{-3}$	-	-
MSP1E3D1 *E. coli* [b]	-	$5.0_{63} \pm 9.0 \times 10^{-3}$	-	-

Entries without values (-) indicates no quantities were obtained. R_s values of PIP_2, Cardiolipin and *E. coli* Nanodiscs were obtained from the averages of other MSP1D1 and MSP1E3D1 Nanodiscs and used for the calculation of Z_{DHH} from the electrophoretic mobilities.

[a] Subscripted numbers are the values used in subsequent calculations, even though they are beyond the precision of the measurements

[b] Lipid content estimated by Avanti Polar Lipids

Table S2
Solvent properties at 20 ^{o}C

Buffer	Conductivity (mS)	Viscosity (cp)
100 mMNaCl, 50 mM Tris pH 7.4	12.0-12.4	1.02_{67}
34 mM NaCl, 17 mM Tris pH 7.4	3.9 - 4.1	1.01_{02}
50 mM NaCl, 25 mM Tris pH 7.4	5.6 - 6.0	1.01_{42}
68 mM NaCl, 34 mM Tris pH 7.4	8.1 - 8.3	1.01_{87}
84 mM NaCl, 42 mM Tris pH 7.4	10.1 - 10.4	1.02_{27}
150 mM NaCl, 75 mM Tris pH 7.4	17.5 - 18.0	1.03_{90}
100 mM NaCl, 50mM Tris, 3 mM $CaCl_2$ pH 7.4	10.0 - 10.5	1.02_{72}
100 mM NaCl, 50mM Tris, 3 mM MgCl pH 7.4	11.8 - 12.3	1.02_{80}
100 mM KCl, 50 mM Tris pH 7.4	14.3 - 14.7	1.01_{60}
100 mM LiCl, 50 mM Tris pH 7.4	9.8 - 10.4	1.04_{21}
1X PBS	13.5 - 13.8	1.02_{00}
100 mM KCl, 50 mM Tris pH 7.4[a]	12.8-13.2	1.10_{90}
100 mM KCl, 50 mM Tris pH 7.4[b]	19.8-21.1	0.71_{90}

Solvent properties of different buffers used to determine the electrophoretic mobility and Z_{DHH} of Nanodiscs by MCE. Experiments, unless denoted, were performed at 20^{o}C.
[a]Conductivity and viscosity values of standard buffer at 25^{o}C
[b]Conductivity and viscosity values of standard buffer at 35^{o}C

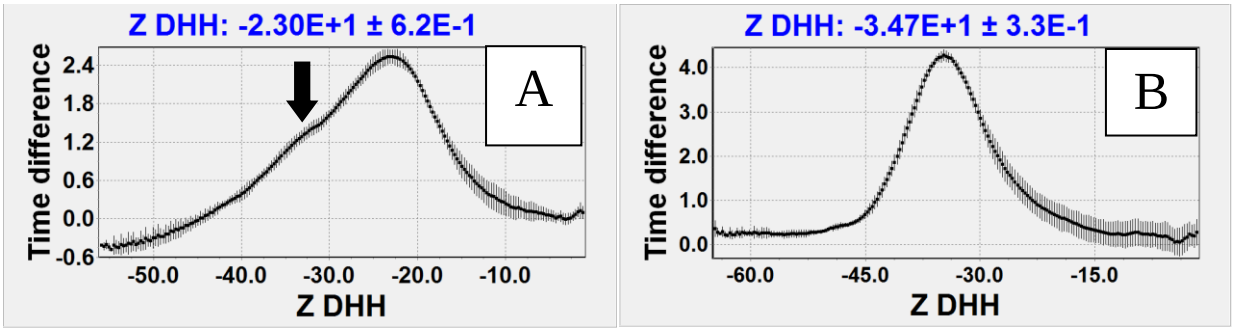

Figures S1 (A) and **S1 (B)** MCE data for MSP1D1 30POPA Nanodiscs in the presence of 3 mM Ca2+ (a) and 3 mM Mg2+ (b). Unlike the distribution data seen in **Figure 1B**, there is a pronounced shoulder (indicated by the arrow) in this data in accord with the aggregation characterized by sedimentation velocity. Similar Z_{DHH} distributions were also observed with 10 and 70POPA Nanodiscs in the presence of Ca^{2+}.

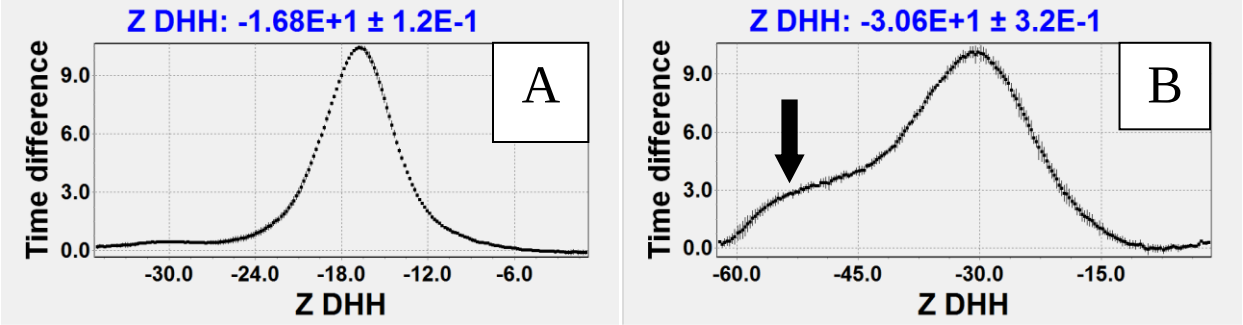

Figure S2 MCE data for MSP1D1 10PIP$_2$ Nanodiscs in the presence of 3 mM Ca^{2+} (**A**) and 3 mM Mg^{2+} (**B**). Unlike the distribution data seen in **Figure 1B**, there is a pronounced shoulder (indicated by the arrow) in the presence of Mg^{2+}. This observation is opposite to that of POPA Nanodiscs, in which POPA Nanodiscs aggregated in Ca^{2+}, but not Mg^{2+}.

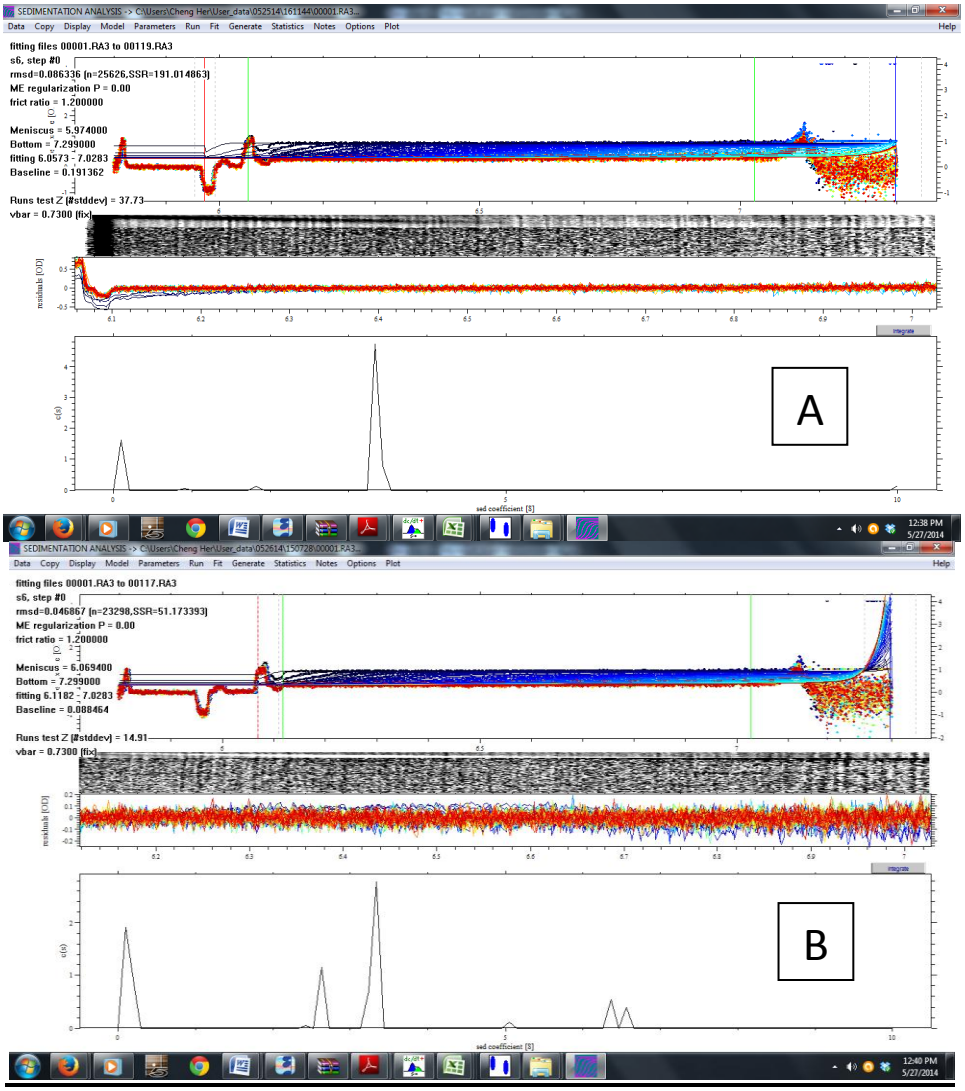

Figure S3 Sedimentation velocity data of MSP1D1 10POPA in the absence (**A**) and presence (**B**) of Ca^{2+}.

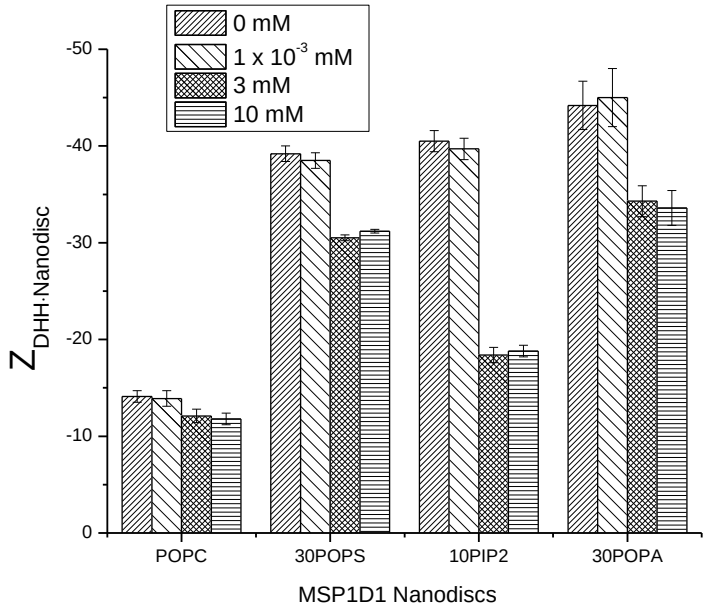

Figure S4 The Z_{DHH} of MSP1D1 POPC Nanodiscs in at varying concentrations of Ca^{2+} (POPC, 30POPS and 10PIP2) and Mg^{2+} (30POPA).

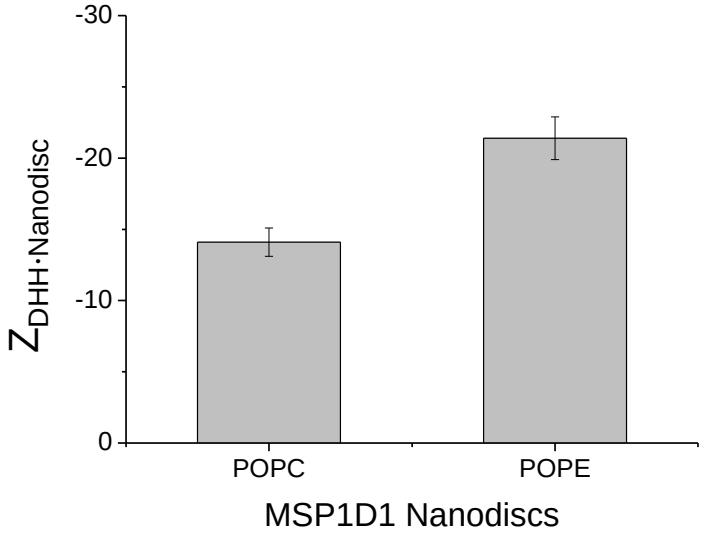

Figure S5 Comparison of Z_{DHH} for MSP1D1 POPC and 10% POPE Nanodiscs.

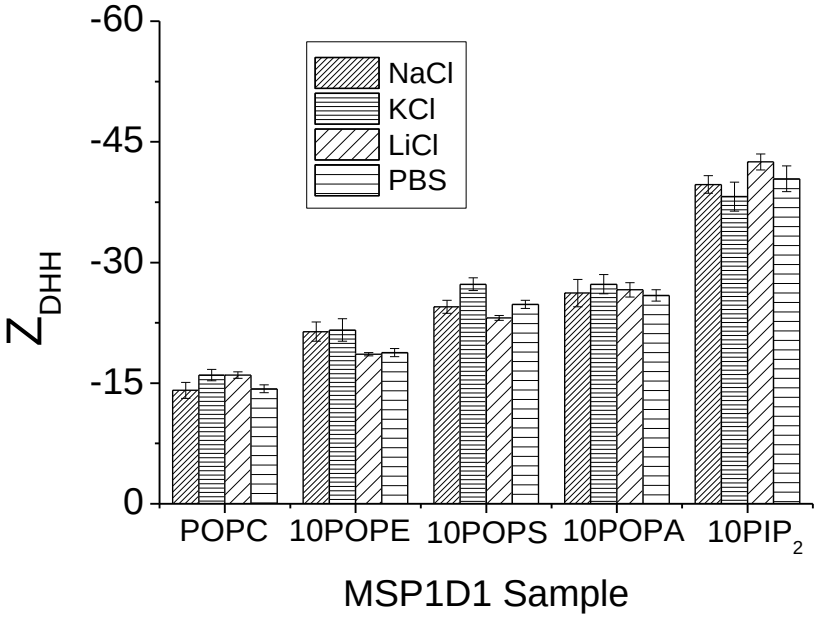

Figure S6 Z_{DHH} of MSP1D1 Nanodiscs in the presence of different monovalent alkali cations.

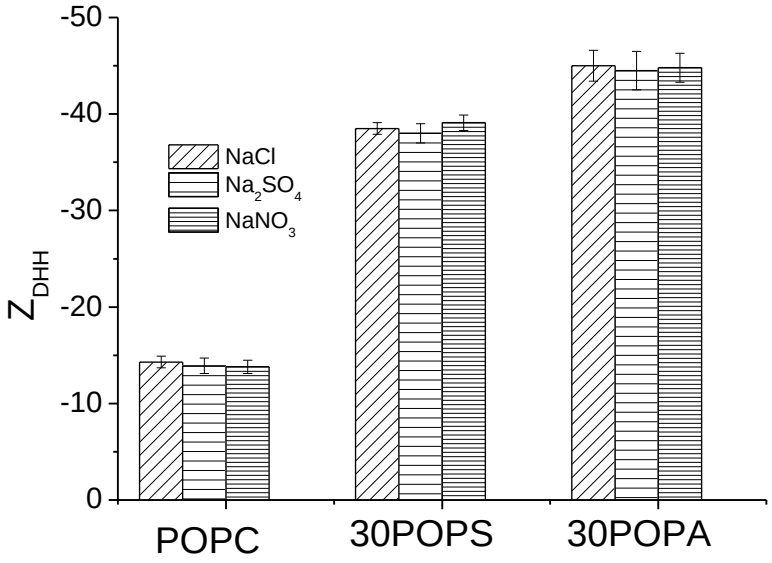

Figure S7 Z_{DHH} of MSP1D1 POPC, MSP1D1 30POPS and MSP1D1 30POPA Nanodiscs in the presence of anions.

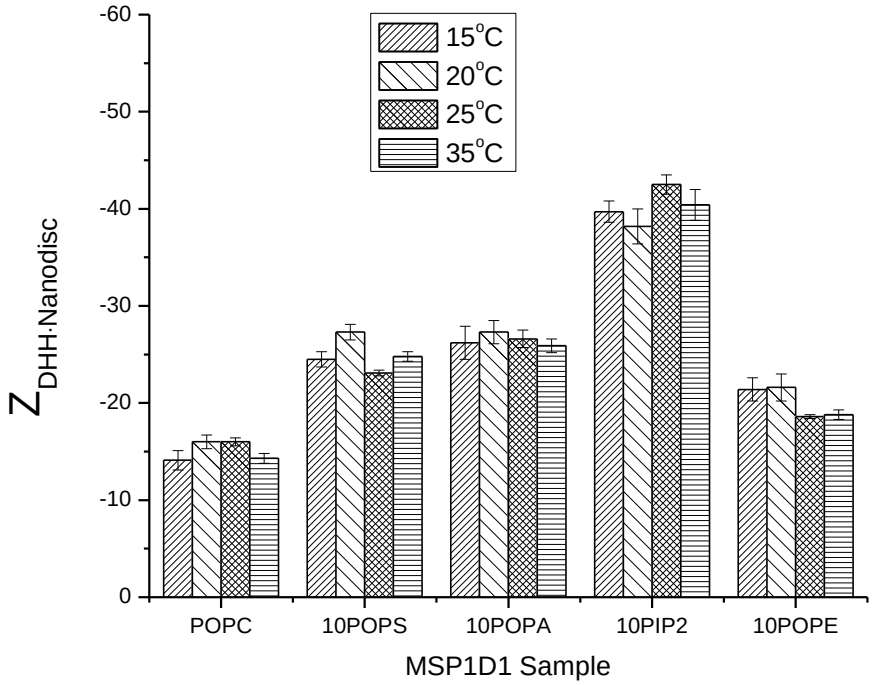

Figure S8 Temperature dependence of Z_{DHH} for POPC, POPS, POPA, PIP_2 and POPE Nanodiscs.

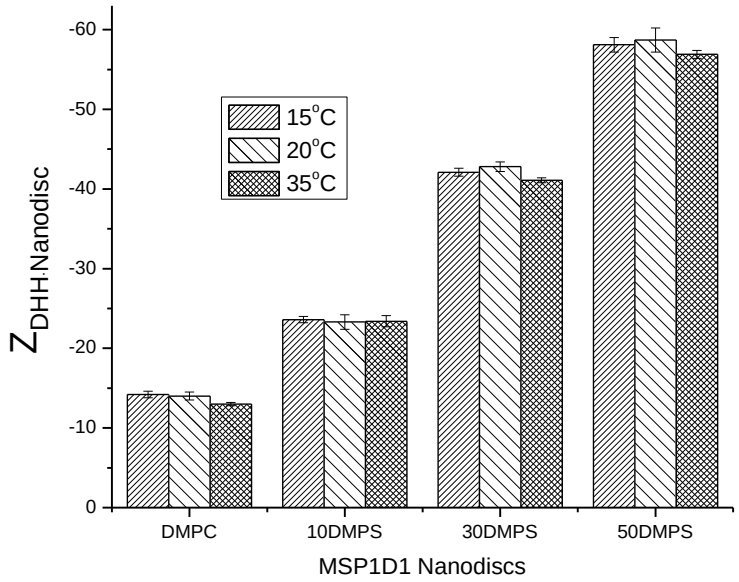

Figure S9 Temperature dependence of Z_{DHH} for DMPC and DMPS Nanodiscs.

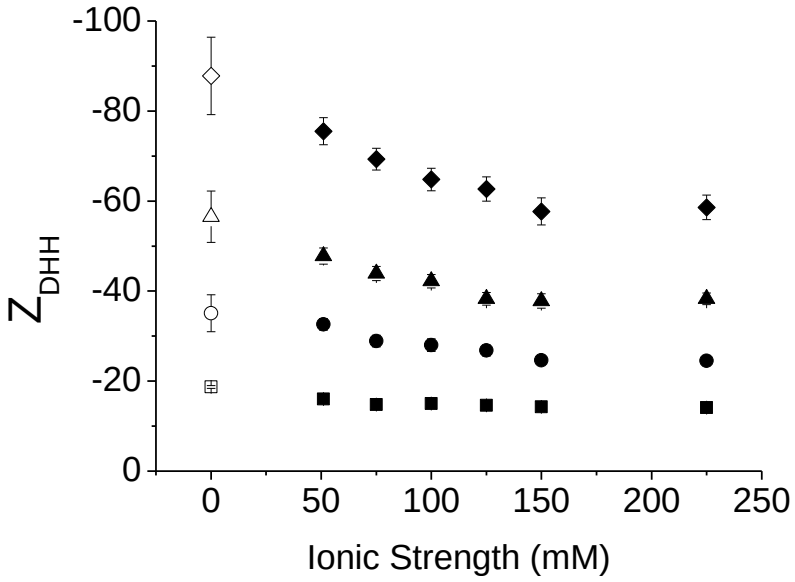

Figure S10 Z_{DHH} as a function of Na^+ concentration for MSP1D1 POPC (■), 10POPS (●), 30POPS (▲)and 70POPS (♦) Nanodiscs. In this figure, the closed data points are the experimental Z_{DHH} values and the open data points are the extrapolated intercept value at zero salt. The data were fit to a 3rd order polynomial in order to generate the extrapolated value at zero salt. The 3rd order provided a significantly better fit (F-test) than a 2nd order polynomial, whereas a 4th order fit provided no improvement over the 3rd order and yielded ill-determined coefficients. Similar observations were made for POPA nand PIP_2 Nanodiscs.

Table S3
Z_{DHH} extrapolated to zero salt

Nanodisc	$Z_{DHH \cdot Nanodisc}$ at zero salt	$Z_{calculated}$[a]
POPC	-18.7 ± 0.3	-16
10POPE	-32.7 ± 2.7	-29
10POPS	-35.1 ± 4.1	-29
30POPS	-56.5 ± 5.7	-54
70POPS	-87.8 ± 8.6	-104
10POPA	-35.9 ± 4.8	-32
30POPA	-69.8 ± 2.0	-63
70POPA	-83.5 ± 5.0	-125
$10PIP_2$	-52.6 ± 2.0	-54

[a] Charge calculated includes the charge calculated for two MSP1D1 MSPs (Z_{DHH} = -16).

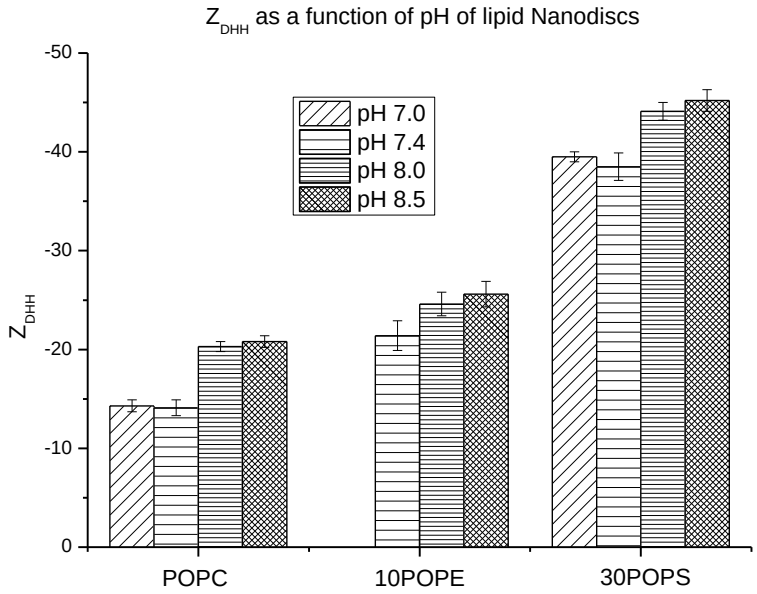

Figure S11 pH dependence of Z_{DHH} for MSP1D1 POPC, MSP1D1 10POPE and MSP1D1 30POPS Nanodiscs. Electrophoretic mobility measurements on 10POPE Nanodiscs at pH 7.0 could not be made. The reason for this is unclear, as sedimentation velocity data on 10POPE Nanodiscs at pH 7.0 show a monodisperse size population. Please note therefore, that in this figure, 10POPE Nanodiscs do not have a Z_{DHH} plotted at pH 7.0.

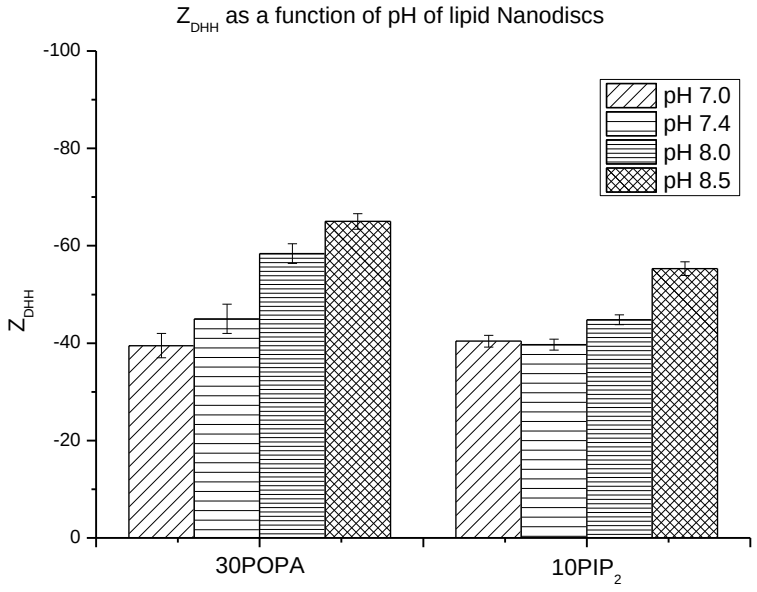

Figure S12 pH dependence of Z_{DHH} for MSP1D1 30POPA and MSP1D1 10PIP_2 Nanodiscs.

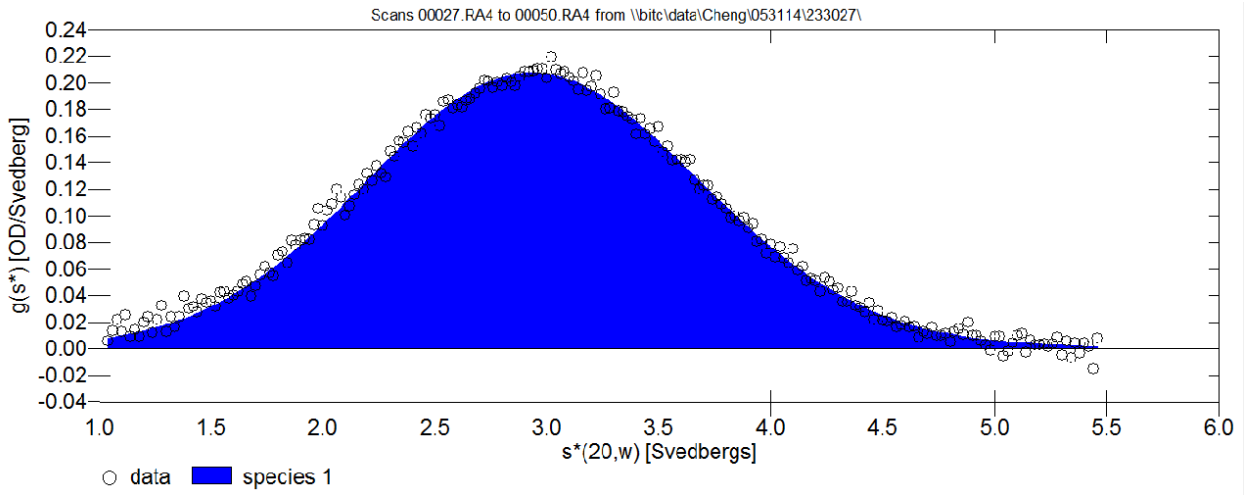

Figure S13 Sedimentation velocity data of 10POPE Nanodiscs in standard buffer at pH 7.4 using DC/DT+ [Philo, 2000].

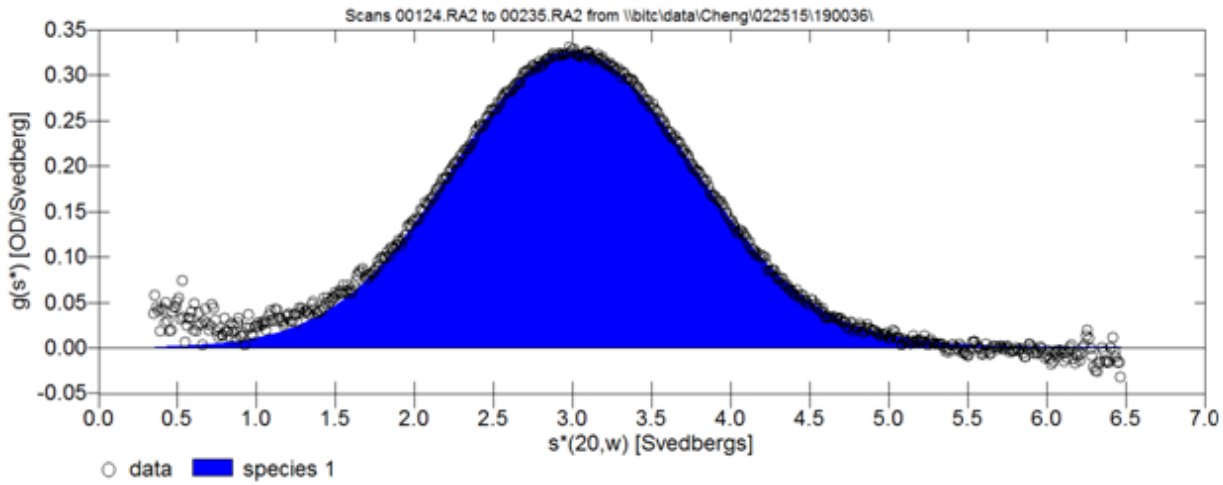

Figure S14 Sedimentation velocity data of 10POPE Nanodiscs in standard buffer at pH 7.0 using DC/DT+ [Philo, 2000].